Machine Learning-based Classification of Hyperspectral Imagery

Mohd Anul Haq[1], Ziaur Rehman[2*], Ahsan Ahmed[3], Mohd Abdul Rahim Khan[1]

[1]Department of Computer Science, College of Computer and Information Sciences,
Majmaah University, Al-Majmaah 11952, Saudi Arabia
[2]Department of Civil and Environmental Engineering, College of Engineering, Majmaah University, Al-Majmaah 11952, Saudi Arabia
[3]Department of Information Technology, College of Computer and Information Sciences,
Majmaah University, Al-Majmaah 11952, Saudi Arabia

*Corresponding Author: Ziaur Rehman, z.rehman@mu.edu.sa

Summary
The classification of hyperspectral imagery (HSI) is essential in the surface of earth observation. Due to the continuous large number of bands, HSI data provide rich information about the object of study; however, it suffers from the curse of dimensionality. Dimensionality reduction is an essential aspect of Machine learning classification. The algorithms based on feature extraction can overcome the data dimensionality issue, thereby allowing the classifiers to utilize comprehensive models to reduce computational costs. This paper assesses and compares two HSI classification techniques. The first is based on the Joint Spatial-Spectral Stacked Autoencoder (JSSSA) method, the second is based on a shallow Artificial Neural Network (SNN), and the third is used the SVM model. The performance of the JSSSA technique is better than the SNN classification technique based on the overall accuracy and Kappa coefficient values. We observed that the JSSSA based method surpasses the SNN technique with an overall accuracy of 96.13% and Kappa coefficient value of 0.95. SNN also achieved a good accuracy of 92.40% and a Kappa coefficient value of 0.90, and SVM achieved an accuracy of 82.87%. The current study suggests that both JSSSA and SNN based techniques prove to be efficient methods for hyperspectral classification of snow features. This work classified the labeled/ground-truth datasets of snow in multiple classes. The labeled/ground-truth data can be valuable for applying deep neural networks such as CNN, hybrid CNN, RNN for glaciology, and snow-related hazard applications.

Keywords:
Hyperspectral, Classification, ANN, Dimensionality

1 Introduction

Snow slip terrain can produce challenging and very dangerous morphologies. Abrupt slopes are perilous from avalanches (Snow slip), rockfalls, or debris flows that make most areas of interest partially or entirely unreachable. In the current scenario, this is the most challenging area of research to deal with the accessibility of isolated points (e.g., avalanche activity prediction, weather measurement, snow summaries, and so on). Most of the terrains isolate without acquiring spatially continuous datasets from satellite remote sensing instruments. The application of remote sensing fills the information gap in the prevailing ground measurement networks and isolated areas. Most research uses the remote sensing data (optical satellite imagery) of snow and avalanche to evaluate the snow cover. The hyperspectral imagery classifications have become the challenging and essential approach in the area of remote sensing. A taxonomy of HSI's has enticed excessive consideration in numerous solicitations, for instance, terrestrial analysis and resource tracking in the arena of remote recognizing. Generally, the compound physiognomies of HSI statistics create the precise taxonomy of such statistics perplexing for modern machine erudition approaches. Snow is one of the most colorful materials and shows variability in reflectance beyond 0.8 µm; fresh snow usually has a high reflectance, whereas wet snow reflectance is lower than fresh snow [1]. The analysis of different snow types is important for glaciological, hydrological, and climatic models. Hyperspectral images provide valuable information about different types of snow. The reason for hyperspectral images being helpful is the detailed spectral information acquired by the sensors at different wavelengths continuously; it helps properly identify the elements and classify them [2], [3]. The classification of hyperspectral images can be problematic for various reasons, such as spatial resolution, dimensionality issues, and limited data for training [4].

Various researchers attempted hyperspectral classification on public datasets such as Salinas-A, Pavia Center, Pavia University, Indian Pines, Kennedy Space Center [5-11]. These public datasets come with readily available labeled/ground-truth datasets, and on the other side, there is no available labeled data for different snow classes. In the current investigation, an attempt was made to contribute significantly to make snow-labeled data that can be used for many AI algorithms for hyperspectral classification.

To deal with the issue of high dimensionality, a couple of methods have proved to be effective: feature extraction and feature selection [12]. Feature extraction could be

Manuscript received April 5, 2022
Manuscript revised April 20, 2022
https://doi.org/10.22937/IJCSNS.2022.22.4.24

achieved using Principal Component Analysis (PCA) or Independent Component Analysis [13]. A previous study has shown that extracting class-specific features can significantly enhance the classification of hyperspectral images [14]. The kernel-based approach has also been found efficient for hyperspectral image classification [15]. The use of multiple attributes such as pixel spectral information, pixel texture and shape features, and dimensionality reduction has also been fruitful for hyperspectral image classification [16]. The traditional methods like minimum distance, k-nearest neighbors were found to be inefficient to get the in-depth features due to the dimensionality issue [17]. Artificial Intelligence (AI) and Machine Learning (ML) techniques were more effective for hyperspectral image classification [18].

AI can be considered the encompassing umbrella for ML, SNN, and DL (Deep Learning). Compared to shallow learning methods, the DL technique has the advantage of building deep architectures to learn more abstract information [19], [20]. The deep architecture consists of several layers; these layers execute to extract different features from the image and classify them. Autoencoders are a family of neural networks appropriate for pattern recognition, essential in classification [21]. An Autoencoder typically takes in unlabeled data as input and tries to reconstruct it as accurately as possible [22]. The Autoencoder has one input layer with n units, one hidden layer of h units, and one reconstruction layer of n units with an activation function f. There are two steps to reconstructing the input data: the first is encoding, and the second is decoding [17], [23].

In this paper, the aim was to study the effectiveness of the JSSSA algorithm for hyperspectral image classification and compare the performance with SNN. Ultimately, the paper focused on: 1) Generating the labeled data for different snow classes in Indian Himalayas. 2) Application of JSSSA for hyperspectral image classification. 3) To assess the high dimension issue, PCA was to reduce them. 4) Both spatial and spectral properties were utilized to classify the data rather than just spectral or spatial individually. 5) Finally, a comparison was made between the results obtained through JSSSA and SNN. JSSSA was used for two tasks: feature extraction and fine-tuning [23].

2 Literature review

The conventional unsupervised FE methods are not suitable for HSI classification. This paper enhances the unsupervised FE approach [24] for HSI classification, including the Neighborhood Preserving Embedding framework. In experimental works, the proposed FE method outperforms the conventional unsupervised methods of HSI classification. Moreover, the proposed

A proposed hybrid approach [27] used unsupervised learning and supervised learning. In the case of unsupervised learning, the knowledge is collected from

method showed better performance than the deep learning-based classification of HIS on spectral-spatial features.

The proposed unsupervised Deep Feature Extraction approach [25] produced better performance over the existing state-of-the-art algorithms, kernel counterpart (kPCA), principal component analysis (PCA) of and some aerial classification. This proposed approach has better efficiency in learning the representations of data. The method applied the single-layer approach of convolution network for high resolution and the detailed result of neighbor pixels. Moreover, it outperforms in the case of single-layer variants and complexity and abstraction level features. The proposed approach used the 3-D Convolutional Autoencoder(3D-CAE) [26] without any training labeling of the samples to extract features in the fashion of unsupervised learning. The models applied the spatial-spectral feature extraction by the unsupervised to extend into the images at the same sensor, producing different images to learn the sensor-specific features. As a result, under the unsupervised measurement, the model learns spatial-spectral features of HSI. The paper showed the benchmarks on datasets of hyperspectral images to extract spatial-spectral features in case of sensor-specific. This model overtook numerous state-of-the-art classifications by the deep learning-based Convolutional neural networks.

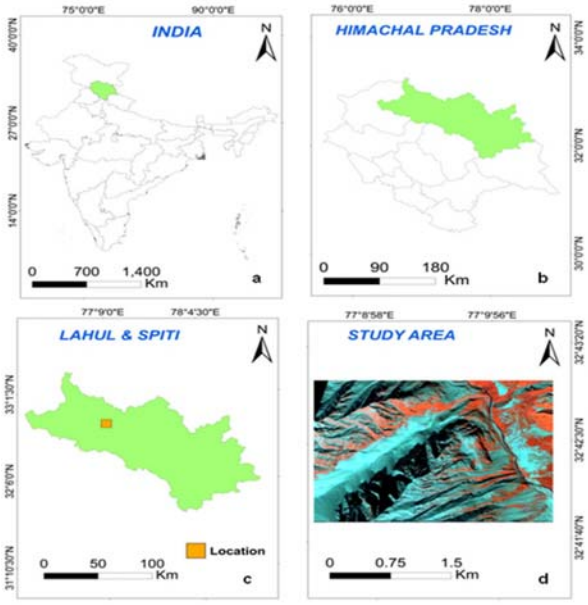

Fig. 1: (a) Map of India. (b) Map of Himachal Pradesh. (c) Lahul and Spiti valley in Himachal Himalayas. The location of AVIRIS-NG used in this study is shown as a small rectangle. (d)AVIRIS-NG image 1 is used in this study.

both types of samples, such as unlabeled and labeled samples, to normalize the supervised learning. Here, it represents two types of branch networks separately to

implement clustering and classification on features. The shared structure is performed the intra-cluster similarity and inter-cluster dissimilarity to embedded into the supervised learning procedure to enhance the generalization capacity. As a result, using the two widely used HSI datasets to show the proposed superior performance.

This paper presents a novel unsupervised feature extraction approach [28] to extract deep-level spatial structure features for HSI classification. Firstly, the authors obtained the deep multilevel spectral-spatial features of the hyperspectral image. Secondly, the unsupervised autoencoder approach reduces the deep spatial features and raw spectral information. The main target of fusion is to fulfill the target of self-supervised learning to detect the necessary amount of information from the input data. In last, the spectral-spatial features fused into multiple scales to evaluate the final discriminative features. The experimental works have shown the effectiveness of the proposed support vector machines algorithm and the methods more essential and effective of hyperspectral image classification. The dataset has fewer training samples with some complexity and heterogeneity in remote sensing space.

The Proposed approach used Deep learning methods to hyperspectral unmixing images [29], and deep learning obtained excessive feature extraction and better performance. Hyperspectral imagery applications play an essential role in Hyperspectral unmixing. Multiple problems are available in deep learning-based spectral unmixing. In the unsupervised autoencoders methods, networks are not sufficient to obtain the deep features. The Autoencoders have limited prior information; due to this problem, this approach used semi-supervised learning to improve performance over the unmixing methods. The modesl used the deep neural network in the absence of a pooling layer. The scale is selected supervised from original input data, which is friendly uses nature and nurture. Experimental work has shown better performance and quantitative results to compare some state-art of existing deep learning unmixing approaches.

3 Study Area and Data Sources

The first study area is Manali, Solang, Dhundi, and surrounding areas in Himachal Pradesh; see Figure 1. Manali (32o 14' N, 77o11' E) is located in Kullu district, Himachal Pradesh, in the region of North-western Himalaya at an elevation around 2,000 meters above sea level (a.s.l.). Dhundi (32o21'N, 77o 7'E) is located at an elevation above 2800 m a.s.l. For the second study area, we collected data from Patsio glacier, which is situated between the geographical coordinates 32o47'40" N; 77o17'57" E to 32o44'40" N; 77o20'59" E in the district of Lahaul-Spiti in the Great Himalayan range. The total length of the glacier is around 3.95 km, and the snout of the glacier is located at an elevation of about 4850 m.a.s.l [30].

In the current study, the AVIRIS-NG dataset was used for classification. AVIRIS-NG has a spatial sample distance ranging between 0.3 to 20 m with a spectral range from 380 nm to 2510 nm wavelength. It has 5 nm spectral sampling [31], [32]. This imaging spectrometer has 224 spectral channels and a 10 nm wide spectral resolution [31]. AVIRIS-NG is better than AVIRIS in terms of spectral resolution, lower signal-to-noise ratio, and greater accuracy compared to AVIRIS [32]. Three levels of products, viz. L0, L1 and L2 were generated from the AVIRIS-NG India campaign. The L0 and L1 data represent raw data, calibrated and orthorectified radiance, respectively, which were generated onboard the aircraft. The L2 data represent surface reflectance products in all the bands after atmospheric correction. L1 data of site ID 159 (dedicated for snow and glaciers in Himachal Pradesh) was used in the current study, which represents calibrated and orthorectified radiance data cubes.

Four snowfield expeditions were carried out from 2016 to 2019 during winter months (Jan and Feb) in the Indian Himalayas using an ASD field spectrometer. The Toikka snow fork was used to collect spectral reflectance and snow properties in synchronization with GPS datasets. A spectral library was developed for different snow types (clean and fresh snow, melting snow, wet snow, dirty snow, and snow under shadow), waterbody, and all remaining classes under non-snow). MATLAB 2019b was used to prepare the labeled dataset for AVIRIS-NG images using a developed spectral library. Making this labeling data was a labor-intensive process since automatic labelers may fail to understand the class label due to several issues such as absorption, scattering, and neighborhood effects with special emphasis on snow. Spatial, spectral, and physical properties were carefully considered with the help of domain experts during the whole image labeling process. Data visualization techniques were used to identify further and remove overlapping classes. The Spectral reflectance graphs for clean snow, wet snow, dirty snow, waterbody, melting snow, snow under the shadow, and non-snow are illustrated in Figure 2.

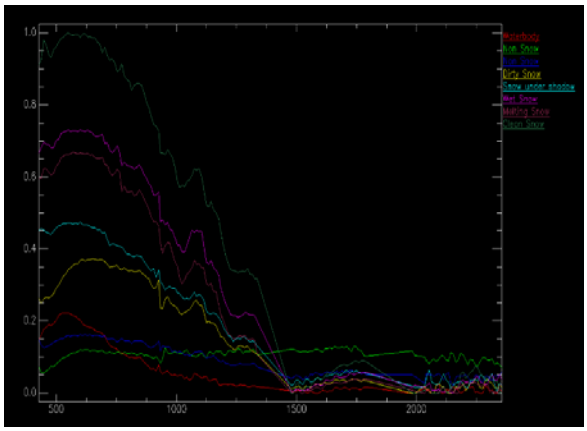

Figure 2: Spectral reflectance graphs for clean snow, wet snow, dirty snow, water body, melting snow, snow under

4 Methodology

4.1 Data Pre-processing

Pre-processing of data is one of the major tasks when working with hyperspectral imagery. Initially, the correction of images to remove noisy bands and zero bands (band 6) in the image took place. Spectral resampling was performed to compare between spectra of AVIRIS NG and ASD spectra. Spectral resampling is also useful for improving the signal-to-noise ratio, which reduces spectral resolution during spectral resampling. The application of local de-stripping methods was applied in the next step. Here, striped values were replaced by the average of the nearest pixel values. To correct the atmosphere influencing factors, the FLAASH module of ENVI software was used. Water vapor absorption bands 194 - 218 (1,343 to 1,463 nm) and 286 - 320 (1,803 to 1,974 nm) were removed. AVIRIS-NG image, which originally had 425 bands, was reduced to 364 after the removal of zero bands and water vapor absorption bands. The methodology followed in this study is illustrated using a flowchart (Fig. 3). The details of snow and ice cover classes are provided (Table 1).

Table 1: Snow and ice cover classes and numbers of pixels in the AVIRIS-NG dataset

Class	Total No. of samples
Clean snow	200
Melting snow	446
Wet snow	353
Dirty snow	93
Snow under shadow	830
Non-snow	1651
Waterbody	77

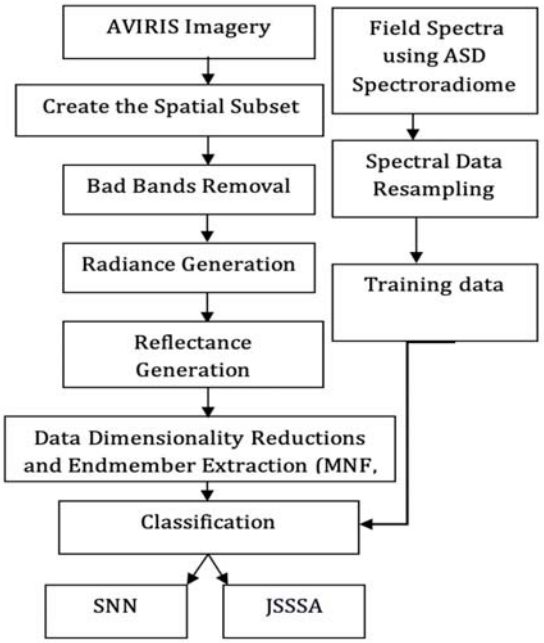

Fig. 3: Flowchart of the methodology used for JSSSA and SNN Classification

Various research split the dataset randomly into training, testing, and validation [17], [33-36] however; the split data ratio plays an important role in assessing the model's validation. K-fold cross-validation is one of the good techniques used for data splitting to avoid overfitting and better generalization of the model. To decide the k in k fold validation, it depends on the size we choose for our test set (e.g. if the testing dataset is 10% or 20% then k value will be 10 or 5 respectively). In the current investigation, we used 5-fold cross-validation. First, the total 3650 samples were shuffled randomly and then divided into 5 groups or 5 folds (730 samples each for each fold). The first fold is treated as a validation set, and the method is fit on the remaining 4 folds. The model was then iteratively trained and validated on these different sets. There were 7 output classes (clean snow, melting snow, wet snow, dirty snow, snow under shadow, non-snow, and water body).

4.2 Joint Spatial-Spectral Stacked Autoencoder Based Classification

An attempt was made in the present investigation to use the JSSSA similar to [17] with some modifications. The modifications were based on the data splitting technique and choice of the activation function. This algorithm first initialized the image parameters as region size, image width, and height (737, 559 pixels) followed by PCA (Fig. 4). Then flattening of the array was done based on exp 2n*1 (where n was the number of principal components).

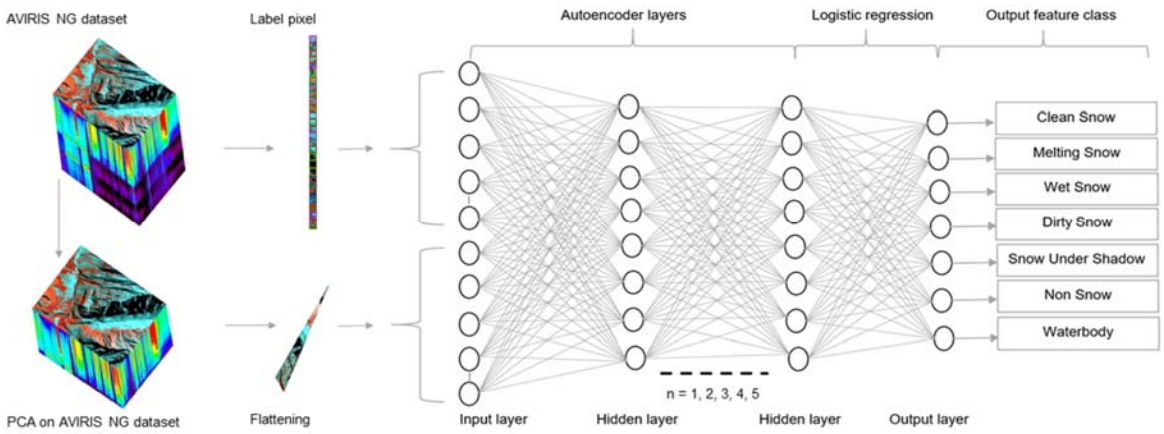

Figure 4: Schematic representation of the spectral and spatial classification of AVIRIS NG data set used in this study. Here Autoencoder with several hidden layers ranging from 1 to 5 was used for feature extraction, and logistic regression was applied for the final classification of output feature classes under observation.

In the next step, concatenation and scaling were performed for matrix M. Then, the image was normalized onto unit interval. After it, the procedure of JSSSA was performed with its parameters. To carry out analysis using DNN, five architectures with hidden layers ranging from 1 to 5 were considered for analysis. The Rectified Linear Unit (ReLU) activation function overcomes the vanishing gradient problem, allowing models to learn faster, perform better, and recommended activation functions for deep neural networks. ReLU is a nonlinear activation function that returns the same value provided as input if the value is greater than 0 (linear behavior); it gives 0 if the provided value is less than 0 (nonlinear behavior); see Eq. (1). The ReLU layer does not change the size of its input.

$$f(x) = \begin{cases} x, x \geq 0 \\ 0, x < 0 \end{cases} \quad (1)$$

Selecting the number of hidden layers and the number of neurons in hidden layers is a crucial challenge in neural networks. Results were assessed based on the kappa coefficient values (Fig. 5). For all five architectures, the algorithm was run with epochs ranging from 100 to 3200 to compute the reconstruction and loss for each epoch. The optimal kappa coefficient value concludes that 4-layer architecture with 100, 100, 50, and 25 neurons in the four layers respectively performed better than other architectures with a kappa coefficient value of 0.946. This maximum Kappa coefficient value for 4-layer architecture remained constant at 0.946 (~ 0.95) after 2700 epochs (Fig. 6.). The initialization of the logistic regression layer was performed by setting the number of input and output neurons followed by probability computation and assignment of the back-propagation algorithm and learning rate.

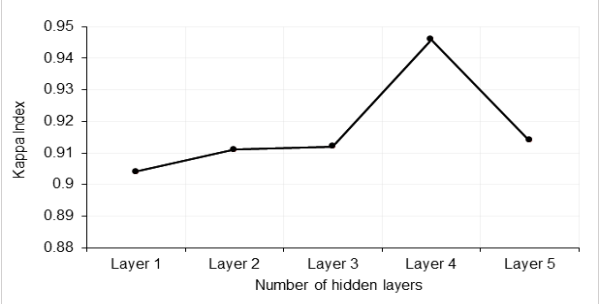

Figure 5: Comparative study of kappa index value concerning the number of layers in the JSSSA.

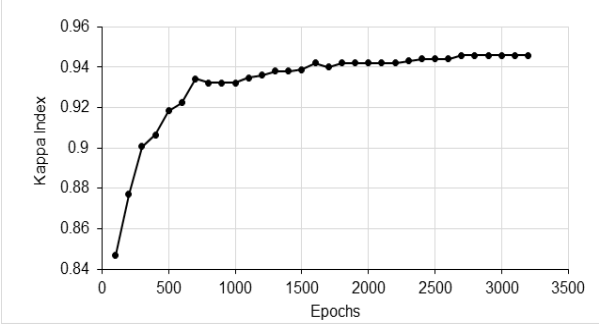

Figure 6: Kappa Index values for JSSSA with 4-layer's architecture with 100 and 100, 50 and 25 neurons in the 4 layers respectively and epochs ranging from 100 to 3200

4.3 Shallow Neural Network Based Classification

To implement SNN for AVIRIS-NG classification, an Adaptive Moment Estimation (ADAM) optimization algorithm was applied. Data was divided using 5-fold cross-validation The k-fold validation assists in choosing the number of neurons in each hidden layer. 2 hidden layer networks were selected with 70 and 35 neurons based on the lowest average testing error over the 5 attempts of candidate dimensionalities using 4 folds as training and the 5th one as testing data. SNN was trained based on 3650 samples, and the training iterations was set to 2,000. There were 364 input bands were used as input nodes which target 7 nodes for 7 snow output classes. A learning rate of 0.002 was found significant with the ADAM optimizer.

4.4 SVM Classification

The primary purpose of SVM is classification, but it is also used for regression statements. A class in support vectors has the maximum distance from the hyperplane. The distance margin defines as the distance between different support vector classes. The sum of D+ and D- calculate as distance margin, where D-, hyperplane has the shortest distance from the closest negative point and D+, hyperplane has the shortest distance from the closest positive point. The main aim of SVM is to find the maximum distance margin, which gives the optimal hyperplane. The optimal hyperplane always gives excellent classification. In the case of non-linear, which produces low and no distance margin, SVM showed misclassification. In that scenario, SVM used the kernel functions to convert the non-linear data into 2D or 3D dimension arrays. The kernel functions convert the minor dimensional feature space into high dimensional feature space.

5 Accuracy Assessment

To measure the competence and compare the results of different techniques, several measurement coefficients like the Kappa coefficient, overall accuracy (OA) and average accuracy (AA) were assessed [39]. Average's accuracy is the ratio of the number of properly classified pixels to the number of reference pixels for the similar class. Overall accuracy is the total number of correctly classified pixels divided by the classes total number of ground pixels. The average's accuracy measurements are also associated with omission and commission errors [40]. The kappa coefficient calculates the agreement between correctly classified pixels' values and ground truth pixels' values. Kappa coefficient (K) is given as equation 2 [41].

$$\frac{N\sum_{i=1}^{r} X_{ii} - \sum_{i=1}^{r}(x_{i+})(x_{+i})}{N^2 - \sum_{i=1}^{r}(x_{i+})(x_{+i})} \quad (2)$$

Where N is the number of observations, X_{ii} is the number of observations in row i and column i (the major diagonal in the confusion matrix), x_{i+} and x_{+i} are the marginal totals of row r and column i, respectively, and r is the number of rows in the matrix.

6. Results and Discussions

The implemented JSSSA extracts more abstract and uniform features that are believed to have higher classification accuracy than traditional shallow classifiers [17], [23]. Classification results from JSSSA and SNN techniques were obtained where the classes are clean snow (clean and fresh snow), melting snow, wet snow, dirty snow, snow under the shadow, waterbody, and remaining all other classes were under non-snow (Figure 7). The overall accuracy of classification was 96.13%, 92.40%, and 82.87% for JSSSA, SNN, and SVM respectively (Table 2, 3 and 4).

Table 2: Confusion matrix and accuracies for JSSSA classification

Confusion Matrix	Clean snow	Melting snow	Wet snow	Dirty Snow	Snow under shadow	Non-Snow	Water body	Row total
Clean snow	50	0	0	0	0	0	0	50
Melting snow	0	88	0	2	2	0	0	92
Wet snow	0	6	74	0	0	0	0	80
Dirty Snow	0	0	0	15	2	0	0	17
Snow under shadow	0	0	2	2	150	4	0	158
Non-Snow	0	3	1	0	4	330	0	338
Waterbody	0	0	0	1	0	0	14	15
Column total	50	97	77	20	158	334	14	750
Agreement/accuracy	100	90.72	96.10	75.00	94.94	98.80	100	
Omission Error	0.00	9.28	3.90	15.00	5.06	1.20	0.00	
Commission Error	0.00	4.35	7.50	11.76	5.06	2.37	6.67	
Overall Accuracy	96.13							
Kappa coefficient	0.95							

The image classification for some classes isn't satisfactory, e.g. dirty snow class shows only 75% accuracy using JSSSA and the same class shows only 48% accuracy using SNN. On the other hand, clean snow classification for both techniques JSSSA and SNN are 100% accurate. This is because albedo ranges around 0.98 for clean/fresh snow but 0.3 for dirty snow in the visible wavelengths [42]. Melting snow has accuracy around 90% and 87% in JSSSA and SNN classification, respectively. The classification of water bodies is also good for both JSSSA and SNN methods, and the rest other classes have accuracies equal to or more than 90%. The Kappa coefficient values were 0.95 and 0.90 for JSSSA and SNN classification. Based on overall accuracy and Kappa values, the JSSSA technique proves to be more efficient than the SNN method. The main issue with the JSSSA technique is the requirement of high-end computing in terms of GPUs (Graphics Processing Unit) or a cluster of GPUs for good computing speed. On the other hand, SNN can effectively work on contemporary CPUs (Central Processing Units).

Table 3: Confusion matrix and accuracies for SNN classification.

Confusion Matrix	Clean snow	Melting snow	Wet snow	Dirty Snow	Snow under shadow	Non-Snow	Water body	Row total
Clean snow	50	0	0	0	0	0	0	50
Melting snow	0	85	2	2	3	0	0	92
Wet snow	0	5	72	2	0	1	0	80
Dirty Snow	0	1	0	13	2	1	0	17
Snow under shadow	0	2	2	5	140	9	0	158
Non-Snow	0	3	6	4	4	321	0	338
Waterbody	0	0	0	1	2	0	12	15
Column total	50	96	82	27	151	332	12	750
Agreement/accuracy	100	87.63	93.51	48.15	92.72	96.69	100	
Omission Error	0	11.46	12.20	51.85	7.28	3.31	0	
Commission Error	0	7.61	10.00	23.53	11.39	5.03	20	
Overall Accuracy	92.4							
Kappa coefficient	0.90							

Table 4: Confusion matrix and accuracies for SVM classification.

Confusion Matrix	Clean snow	Melting snow	Wet snow	Dirty Snow	Snow under shadow	Non-Snow	Water body	Row total
Clean snow	40	0	7	0	0	3	0	50
Melting snow	0	80	5	2	3	2	0	92
Wet snow	1	5	62	2	5	1	4	80
Dirty Snow	4	1	0	9	2	1	0	17
Snow under shadow	0	3	2	1	128	16	8	158
Non-Snow	5	3	6	4	4	316	0	338
Waterbody	0	0	0	1	2	2	10	15
Column total	50	92	82	19	144	341	22	750
Agreement/accuracy	90	87.63	77.5	52.94	81.01	93.49	66.67	
Omission Error	80.00	86.96	75.61	47.37	88.89	92.67	45.45	
Commission Error	10	11.73	15.98	38.98	18.52	9.65	28.93	
Overall Accuracy of SVM	82.87							
Kappa coefficient	0.81							

Manuscript received April 5, 2022
Manuscript revised April 20, 2022
https://doi.org/10.22937/IJCSNS.2022.22.4.24

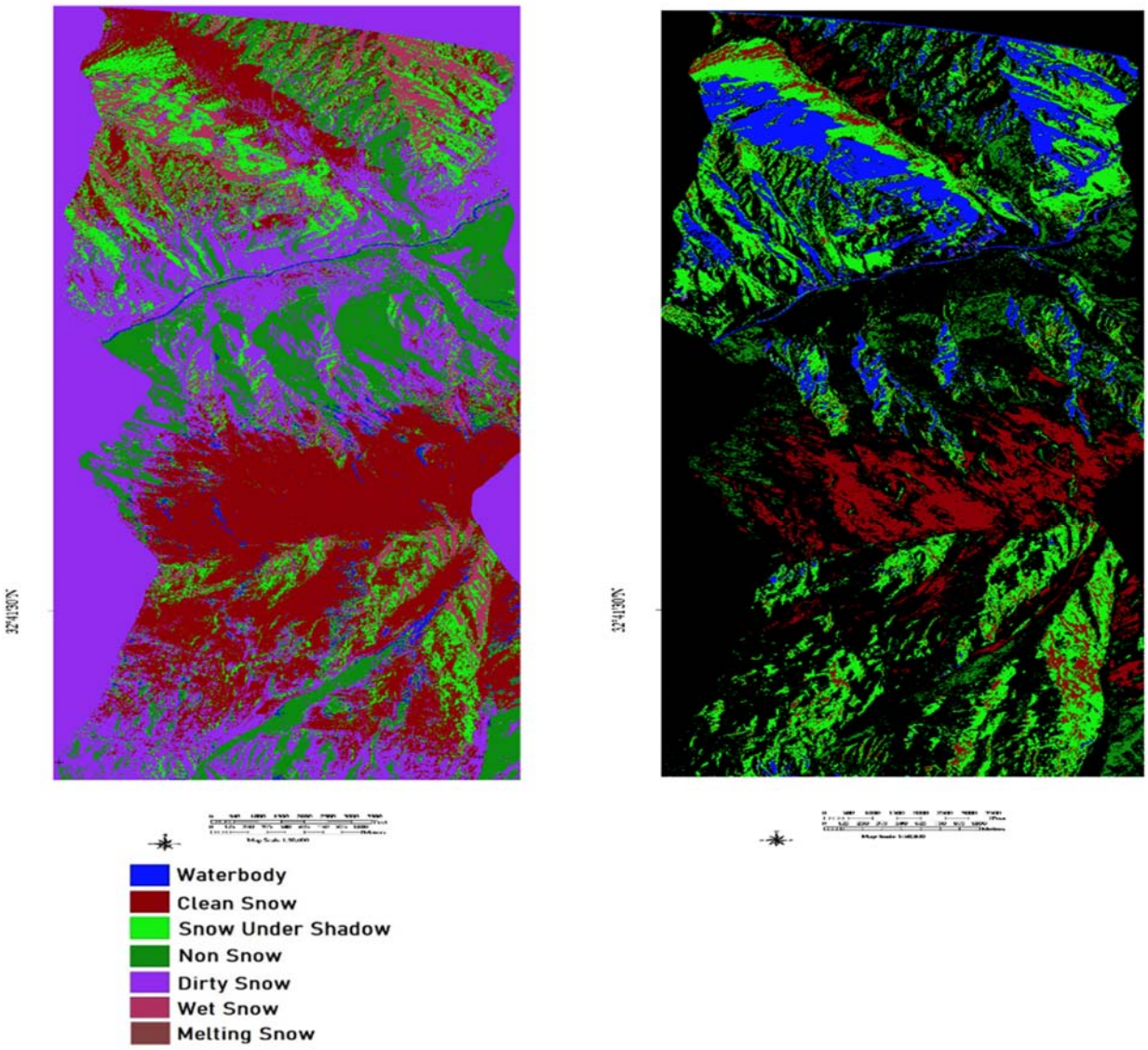

Figure 7 Original image of the study area, classified images (b) JSSSA, (c) SNN, and (d) SVM.

6 Conclusions

In this study, an attempt was made to generate the labeled data for different types of snow classes and assess the performance of JSSSA and SNN techniques on an airborne hyperspectral image of AVIRIS-NG. It was observed that the JSSSA based technique outperforms the SNN technique with an overall accuracy of 96.13% and Kappa coefficient value of 0.95. SNN also achieved a promising accuracy of 92.40% and a Kappa value of 0.90. Both JSSSA and SNN techniques have shown 100% accuracy for clean snow and water bodies. The reason for better classification of clean snow is related to high albedo which makes it separable from other classes in the visible region. The current study suggests that both JSSSA based technique and SNN prove to be an efficient method for hyperspectral classification of snow features. The future scope of the present research is to extend the ground truth data and apply other deep neural architectures such as CNN, hybrid CNN, RNN, etc., in the context of the Himalayas.

Acknowledgment: Ziaur Rehman would like to thank the Deanship of Scientific Research at Majmaah University for supporting this work under Project No. R-2022-10.

Funding Statement: Ziaur Rehman would like to thank the Deanship of Scientific Research at Majmaah University for supporting this work under Project No. R-

Manuscript received April 5, 2022
Manuscript revised April 20, 2022
https://doi.org/10.22937/IJCSNS.2022.22.4.24

2022-10.

References

1. J. Dozier, G. Robert, A. Nolin and T. Painter,: *Interpretation of snow properties from imaging spectrometry, Remote Sensing of Environment,* vol. 113 (4), pp. 25-37, (2013)
2. M. A. Haq,: *Comparative analysis of hyperspectral and multispectral data for mapping snow cover and snow grain size,* The International Archives of the Photogrammetry, Remote Sensing and Spatial Information Sciences, vol. 8 (499), pp 1-6, (2014)
3. B. Hosseiny and R. Shah-Hosseini,: *A hyperspectral anomaly detection framework based on segmentation and convolutional neural network algorithms,* International Journal of Remote Sensing, vol. 41 (18), pp. 6946-6975, (2020)
4. T. A. Moughal,: *Hyperspectral image classification using support vector machine,* Journal of Physics: Conference Series, vol. 439(42) , pp. 882-885, (2013)
5. J. Yue, W. Zhao, S. Mao and H. Liu,: *Spectral-spatial classification of hyperspectral images using deep convolutional neural networks,* Remote Sensing Letters, vol. 6 (6), pp. 468–477, (2015)
6. L. Pan, H. C. Li, Y. J. Deng, F. Zhang, X. D. Chen and Q. Du,: *Hyperspectral dimensionality reduction by tensor sparse and low-rank graph-based discriminant analysis,* Remote Sensing, vol. 9 (452), pp. 1-20, (2017)
7. S. Yu, S. Jia and C. Xu,: *Convolutional neural networks for hyperspectral image classification,* Neurocomputing, vol. 219, pp. 88-98, (2017)
8. J. Xu, H. Li, P. Liu and L. Xiao,: *A Novel Hyperspectral Image Clustering Method with Context-Aware Unsupervised Discriminative Extreme Learning Machine,* IEEE Access, vol. 6, pp.16176-16188. (2018)
9. R. Hang, Q. Liu, D. Hong and P. Ghamisi,: *Cascaded Recurrent Neural Networks for Hyperspectral Image Classification,* IEEE Transactions on Geoscience and Remote Sensing, vol. 57, no. 8, pp. 5384-5394, (2019)
10. X. Zhao, Liang, A. J. X. Guo and F. Zhu,: *Classification of smallscale hyperspectral images with multi-source deep transfer learning.* Remote Sensing Letters, vol. 11 (4), pp. 303-312, (2020)
11. Q. Sun and S. Bourennane,: *Hyperspectral image classification with unsupervised feature extraction,*" Remote Sensing Letters, vol. 11 (5), pp. 475-484, (2020)
12. J. Tang, S. Alelyani and S. Liu,: *Feature Selection for Classification: A Review, Data Classification: Algorithms and Applications,* CRC Press, pp. 1-29, (2014)
13. A. Agarwal, T. El-Ghazawi, H. El-Askary and J. Le-Moigne,: *Efficient hierarchical-PCA dimension reduction for hyperspectral imagery,* in Proc. ISSPIT, Giza, Egypt, pp. 1077-1080, (2007)
14. S. Kumar, J. Ghosh and M. M. Crawford,: *Best-bases feature extraction algorithms for classification of hyperspectral data,* IEEE Transactions on Geoscience and Remote Sensing, vol. 39 (7), pp. 1368-1379, (2001)
15. G. Camps-Valls and L. Bruzzone,: *Kernel-based methods for hyperspectral image classification,* IEEE Transactions on Geoscience and Remote Sensing, vol. 43 (6), pp. 1351-1362, (2005)
16. L. Zhang, L. Zhang, D. Tao and X. Huang,: *On combining multiple features for hyperspectral remote sensing image classification,* IEEE Transactions on Geoscience and Remote Sensing, vol. 50 (7), pp. 879-893, (2012)
17. Y. Chen, Z. Lin, X. Zhao, G. Wang and Y. Gu,: *Deep Learning-Based Classification of Hyperspectral Data,* IEEE Journal of Selected Topics in Applied Earth Observations and Remote Sensing vol. 7 (6), pp. 2094-2107, (2014)
18. A E. Maxwell, T. A. Warner and F. Fang,: *Implementation of machine-learning classification in remote sensing: an applied review,* International Journal of Remote Sensing, vol. 39 (9), pp. 2784-2817, (2018)
19. M. Coşkun, Ö. Yildirim, A. Uçar and Y. Demir,: *An Overview of Popular Deep Learning Methods,* European Journal of Technology, vol. 7 (2), pp. 165–176, (2017)
20. G. Ososkov and P. Goncharov,: *Shallow and deep learning for image classification,* Optical Memory and Neural Networks, vol. 26 (4), pp. 221–248, (2017)
21. A. Voulodimos, N. Doulamis, A. Doulamis and E. Protopapadakis,: *Deep Learning for Computer Vision: A Brief Review,* Computational Intelligence and Neuroscience, vol. 2018 (7068349), pp. 1-13, (2018)
22. M. Peychev, P. Veličković, and P. Liò,: *Quantifying the Effects of Enforcing Disentanglement on Variational Autoencoders,* in Proc. NIPS 2017, California, USA, (2017)
23. Y. Chen, X. Zhao and X. Jia,: *Spectral-spatial classification of hyperspectral data based on deep belief network,* IEEE Journal of Selected Topics in Applied Earth Observations and Remote Sensing vol. 8 (6), pp. 2381-2392, (2015)
24. J. Feng, and J. Zhang,: *Unsupervised Feature Extraction in Hyperspectral Image Based on Improved Neighborhood Preserving Embedding,* In Proc. IGARSS, pp. 1291-1294, Jia Feng, Junping Zhang, Harbin Institute of Technology, China, (2020)
25. A. Romero, C.Gatta, and G. Camps-Valls,: *Unsupervised deep feature extraction for remote sensing image classification,* IEEE Transactions on Geoscience and Remote Sensing, vol. 54 (3), pp.1349-1362, (2015)
26. J. Ji, S.Mei, J. Hou, X. Li, and Q. Du,: *Learning sensor-specific features for hyperspectral images via 3-dimensional convolutional autoencoder,* In Proc. IGARSS , pp. 1820-1823, United States, (2017)
27. Zhang, J., Wei, W., Zhang, L. and Zhang, Y.: *Improving hyperspectral image classification with unsupervised knowledge learning*. In Proc. IGARSS , pp. 2722-2725, Yokohama, Japan, July, (2019)
28. M. Liang, L.Jiao, S. Yang, F. Liu, B. Hou, and H. Chen,: *Deep multiscale spectral-spatial feature fusion for hyperspectral images classification*, IEEE Journal of Selected Topics in Applied Earth Observations and Remote Sensing, vol. 11 (8), pp.2911-2924, (2018)
29. J. Bai, R.Feng, L. Wang, H.Li, F. Li, Y.Zhong, and L. Zhang,: *Semi-Supervised Hyperspectral Unmixing with Very Deep Convolutional Neural Networks,* In Proc. IGARSS , pp. 2400-2403 , Waikoloa, HI, USA , (2020)
30. S. Singh, R. Kumar and A. P. Dimri,: *Mass Balance Status of Indian Himalayan Glaciers: A Brief Review,* Frontiers in Environmental Science, Vol 6 (30), pp. 1-9, (2018)

31. L. Hamlin, R. O. Green, P. Mouroulis, P. Eastwood, Michael, D. Wilson, M. Dudik and C. Paine,: *Imaging Spectrometer Science Measurements for Terrestrial Ecology: AVIRIS and New Developments,* In Proc. AERO'11, Washington DC, USA, pp. 1 – 7, (2011)
32. A. K. Thorpe, C. Frankenberg, A. D. Aubrey, D. A. Roberts, A. A. Nottrott, T. A. Rahn, J. A. Sauer, M. K. Dubey, K. R. Costigan, C. Arata and A. M. Steffke,: *Mapping methane concentrations from a controlled release experiment using the next generation airborne visible/infrared imaging spectrometer (AVIRIS-NG),* Remote Sensing of Environment, vol. 179, pp. 104–115, (2016)
33. M. A. Haq, K. Jain and K. P. R. Menon,: *Modelling of Gangotri glacier thickness and volume using an artificial neural network,* International Journal of Remote Sensing, vol. 35 (16), pp. 6035-6042, (2014)
34. M. A. Haq and M. F. Azam: *Application of Artificial Neural Networks for Glacier Thickness Estimation in the Western Himalayas, India,* In Proc. NCHC-2017, Banglore, India, pp. 17-22, (2017)
35. M. A. Haq, A. Ghosh, G. Rahaman and P. Baral,: *Artificial neural network-based modeling of snow properties using field data and hyperspectral imagery,* Natural Resource Modeling, vol. 32 (4), pp. 1-36, (2019)
36. R. Srinet, S. Nandy, H. Padalia, S. Ghosh, T. Watham, N. R. Patel and P. Chauhan,: *Mapping plant functional types in Northwest Himalayan foothills of India using random forest algorithm in Google Earth Engine,* International Journal of Remote Sensing, vol. 41 (18), pp. 1-14, (2020)
37. I. Good fellow, Y. Bengio and A. Courville,: *Deep Learning (Adaptive Computation and Machine Learning series),* The MIT Press, ISBN 0262035618, (2019)
38. K. Xu, J. Ba, R. Kiros, K. Cho, A. Courville, R. Salakhutdinov, R. Zemel and Y Bengio,: *Show, Attend and Tell: Neural Image Caption Generation with Visual Attention*, In International conference on machine learning, pp. 2048-2057. PMLR, (2015)
39. D. Thompson and S.D., Walter,: *A reappraisal of the Kappa coefficient,* Journal of Clinical Epidemiology, vol. 41, pp. 949–958, (1988)
40. L. Boschetti, S. Flasse and P. Brivio,: *Analysis of the conflict between omission and commission in low spatial resolution dichotomic thematic products: The Pareto Boundary,* Remote Sensing of Environment, vol. 91, pp. 280-292, (2004)
41. J. Sim and C.C. Wright,: *The Kappa Statistic in Reliability Studies: Use, Interpretation, and Sample Size Requirements,* Physical Therapy, vol. 85 (3), pp. 257–268, (2005)
42. J. M. Cook, A. Hodson, A. J. Taggart, S. H. Mernild and M. Tranter,: *A predictive model for the spectral bioalbedo of snow,* Journal of Geophysical Research Earth Surface, vol. 122, pp. 434–454. (2017)
43. Xi. Kan, Y. Zhang, L. Zhu, L. Xiao, J. Wang, W. Tian and H. Tan,: *Snow cover mapping for mountainous areas by fusion of MODIS L1B and geographic data based on stacked denoising auto-encoders,* Computer Materials and Continua, vol. 57 (1), pp. 49–68, (2018)

MOHD ANUL HAQ earned a Ph.D. from Indian Institute of Technology Roorkee, India, in 2013. He received a master's degree in Computer Applications from UP Technical University (currently Dr. A.P.J. Abdul Kalam Technical University Uttar Pradesh) and bachelor's degree from HNB Garhwal University, Uttarakhand. The central component of his research is in artificial intelligence and machine learning. The target applications of his research are deep learning-based image classification, modeling, and forecasting.

ZIA UR REHMAN earned M. TECH. degree in Civil Engineering from Aligarh Muslim University, India, in 2006. He received bachelor's degree in chemical engineering from H.B.T.I. Kanpur, India 2003. From 2007 to 2010 He was associated with HCST, Mathura, India. Since 2011, he has been working as a lecturer in the Department of Civil and Environmental Engineering, College of Engineering, Majmaah University, Al-Majmaah, Kingdom of Saudi Arabia. He had 15 years of experience in teaching. His research interests include wastewater treatment and solid waste management.

AHSAN AHMED earned his master's degree in Computer Science from Jamia Hamdard University, New Delhi, India, in 2008. From 2008 to 2010, he worked at CSIR's laboratory. Since November 2010, he has been working as a lecturer in the Department of Information Technology, College of Computer and Information Sciences, Majmaah University, Al-Majmaah, Kingdom of Saudi Arabia. He had 11 years of experience in teaching. His research interests include machine learning, web technologies, cloud computing, and decision making.

MOHD ABDUL RAHIM KHAN received the M. Tech. degree in information technology from GGSIP University, in 2008. He worked as a Lecturer with Majmaah University, Saudi Arabia. He is currently a Ph.D. Scholar with Lingayas Vidyapeeth, Fridabad, India. His research interests include cybersecurity, computer network security, and information security.